



# Reduction and precipitation of aqueous europium (III) under an air atmosphere by near-infrared femtosecond laser pulses

メタデータ	言語: en 出版者: Elsevier 公開日: 2024-03-06 キーワード (Ja): キーワード (En): 作成者: Tamejima, Kazuya, Mizuta, Chihiro, Nakashima, Nobuaki, Sakota, Kenji, Shinoda, Satoshi, Yatsunashi, Tomoyuki メールアドレス: 所属:
URL	<a href="http://hdl.handle.net/10466/0002000445">http://hdl.handle.net/10466/0002000445</a>

# Reduction and Precipitation of Aqueous Europium (III) under an Air Atmosphere by Near-Infrared Femtosecond Laser Pulses

*Kazuya Tamejima, Chihiro Mizuta, Nobuaki Nakashima, Kenji Sakota, Satoshi Shinoda,  
and Tomoyuki Yatsunami\**

Department of Chemistry, Graduate School of Science, Osaka City University, 3-3-138  
Sugimoto, Sumiyoshi, Osaka 558-8585 Japan

\*To whom correspondence should be addressed. Telephone: +81-6-6605-2554. FAX:  
+81-6-6605-2522. E-mail: tomo@sci.osaka-cu.ac.jp (T.Y.)

## **Abstract**

To meet growing demands for the separation and recycling of rare-earth elements, photo-assisted reduction followed by precipitation is increasingly recognized as a viable non-contact approach. However, only limited light sources are currently available for these processes, because most research has focused on excitation of redox active charge-transfer bands of lanthanoid ions in the VUV and/or UV region. In this study, we carry out the reduction of  $\text{Eu}^{3+}$  to  $\text{Eu}^{2+}$  with hydrated electrons generated in water by near-infrared femtosecond laser pulses under an air atmosphere. The reduction yields are not linearly dependent on either the laser power or the concentration of 2-propanol acting as a hydroxyl radical scavenger. Addition of sulfate ions precipitates  $\text{Eu}^{2+}$  as an insoluble

EuSO<sub>4</sub> after a certain induction time. The absorption/extinction spectroscopy and transmittance measurements reveal the reduction of Eu<sup>3+</sup> and growth of sulfates during the induction time. The success of precipitation by a valence change in water under an air atmosphere opens an avenue for the practical use of near-infrared light for the treatment of lanthanoid elements.

## 1. Introduction

Separation and recycling of rare metals are important issues for the establishment of a sustainable and green society [1]. Europium is one of the critical lanthanoids in modern technology, and its recovery from end-of-life components has been increasingly recognized as a secondary source [2]. There are several approaches to separate lanthanoids, including physical, chemical, electrochemical, and photochemical procedures [3-5]. In the case of europium, photoreduction followed by precipitation [6-10] or chromatography [11] has been proposed for the separation of europium ions from other lanthanoid ions. For the approach using precipitation, the separation of europium relies on the difference of solubility between the Eu<sup>2+</sup> species and the corresponding Eu<sup>3+</sup> species. For example, the solubility of EuSO<sub>4</sub> in water is three orders of magnitude lower than that of Eu<sub>2</sub>(SO<sub>4</sub>)<sub>3</sub> [9]. A variety of light irradiation setups have been examined. Conventionally, low-pressure and/or medium-pressure mercury lamps that show strong line emissions at 184.9 and 253.7 nm have been used to excite the charge-transfer band of Eu<sup>3+</sup>. Although the reduction and precipitation using such light sources have been successful, there remain some problems to be resolved for the practical use of photochemistry for europium recovery. First, the photoreduction using VUV and/or UV light might be hindered, if contaminants in a reactant solution have strong absorption at

those wavelength regions. Second, not only long reaction time but also long induction time before the start of  $\text{EuSO}_4$  precipitation —e.g., 5–30 hours depending on the irradiance—has been reported using mercury lamps [8]. Third, monochromatic light has rarely been utilized, and thus the quantum yields of reduction and precipitation, which are indispensable to compare the efficiency, have not been obtained. Nevertheless, much fundamental knowledge for the optimization of reactions has been accumulated using several hydroxyl radical scavengers [9, 12] and various solvents [6].

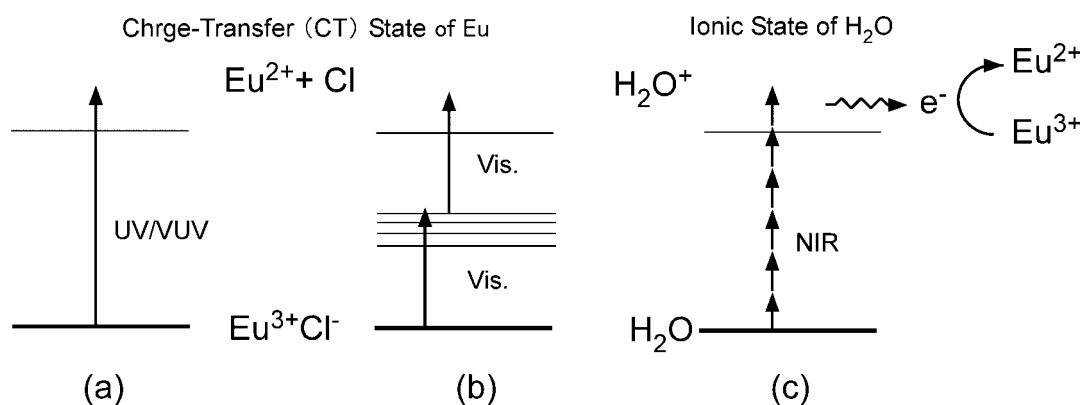


**Fig. 1.** Reduction of  $\text{Eu}^{3+}$  via a charge-transfer (CT) state by (a) a single photon excitation using an UV/VUV laser pulse and by (b) resonant two-photon excitation using visible laser pulses. (c) Reduction of  $\text{Eu}^{3+}$  by hydrated electrons ejected from the ionic state of water generated by nonresonant multiphoton ionization using near-infrared (NIR) laser pulses.

In contrast to conventional lamps, a pulsed laser, which is recognized as a monochromatic light with high-photon flux, is a promising light source, if the absorption wavelength of target elements and emission wavelength of the laser are overlapped. Three processes to change the valence of europium ions are shown in Fig. 1. We previously demonstrated the first approach, which is to reduce  $\text{Eu}^{3+}$  by exciting the charge-transfer (CT) band in degassed alcohol with nanosecond laser pulses of VUV or UV wavelength

(Fig. 1a) [13, 14]. The quantum yield of  $\text{Eu}^{3+}$  reduction by direct single-photon excitation to CT state using UV laser pulse (308 nm) was almost unity [13]. This procedure has been shown to be effective for not only lanthanoid ions but also noble metal ions dissolved in radioactive waste solution [15-18]. The second strategy for changing the valence of  $\text{Eu}^{3+}$  is resonant two-photon excitation to CT state via the f-f transition using visible laser pulses (Fig. 1b). We have found two photon reduction of  $\text{Eu}^{3+}$  to  $\text{Eu}^{2+}$  in nano- and picosecond pulse excitations [19, 20]. The reduction efficiencies of  $\text{Eu}^{3+}$  were largely improved from on the order of  $10^{-5}$  to 1 by picosecond pulse excitation. The improvement would be largely reinterpreted by the simple reasons of pulse shortening. The laser intensity should have increased  $1 \times 10^4$  times by the shortening pulses from 20 ns to 2 ps under the same focusing conditions. The third procedure is the reduction of lanthanoid ions with electrons ejected from solvent by nonresonant multiphoton ionization using focused near-infrared (NIR) femtosecond laser pulses (Fig. 1c) [21-23]. Lanthanoid ions were successfully reduced in degassed alcohol using this approach. Our experiences show that the one-electron reduction of  $\text{Sm}^{3+}$  in degassed alcohol is the case of the ion with the most negative reduction potential ( $-1.55$  V vs. SHE) [22]. However, it should be mentioned that this procedure has not been applied under either an aerated condition or in water. We have reported that noble metal ions ( $\text{Au}^{3+}$ ,  $\text{Ag}^+$ ,  $\text{Pd}^{2+}$ ) are easily reduced in aerated water followed by nanoparticle production [23-25]. In the cases of iron ions, the reduction of  $\text{Fe}^{3+}$  to  $\text{Fe}^{2+}$  (the reduction potential was 0.771 V vs. SHE) in water was dependent on the laser wavelength: via a two-photon absorption process ( $0.8 \mu\text{m}$ ) or by solvated electrons ( $1.2 \mu\text{m}$ ) [24]. For the practical use of the third procedure for the recovery of lanthanoid, it is necessary to carry out the reduction and precipitation of lanthanoid ion in water under an aerated condition.

In this study, we succeed in reducing  $\text{Eu}^{3+}$  to  $\text{Eu}^{2+}$  by hydrated electrons generated by nonresonant multiphoton ionization of water under an air atmosphere using NIR femtosecond laser pulses. The addition of 2-propanol (2-PrOH), a hydroxyl radical scavenger, is the key to performing the reduction of  $\text{Eu}^{3+}$  in water. Absorption/extinction spectroscopy and transmittance measurements reveal the time evolution of the reduction of  $\text{Eu}^{3+}$  and precipitation of  $\text{Eu}^{2+}$  as sulfate.

## 2. Materials and methods

$\text{EuCl}_3 \cdot 6\text{H}_2\text{O}$  (Aldrich, 99.99%),  $\text{EuCl}_2$  (Aldrich, 99.99%), and  $(\text{NH}_4)_2\text{SO}_4$  (Nacalai,  $\geq 99.5\%$ ) were used without further purification. 2-Propanol (2-PrOH, Nacalai, spectral grade,  $\geq 99.7\%$ ) and distilled water (Nacalai) were used as received.

Femtosecond laser pulses (0.8  $\mu\text{m}$ , 40 fs,  $< 0.4$  mJ, 1 kHz) were delivered from a Ti:Sapphire laser (Alpha 100/1000/XS hybrid; Thales Laser). Details of the laser experiments have been described elsewhere [25]. The laser beam was focused on the central part of a quartz cuvette (10 $\times$ 10 $\times$ 40 mm<sup>3</sup>) by using a planoconvex quartz lens with a focal length of 50 mm. The solution (1 or 3 cm<sup>3</sup>) was stirred by a Teflon-coated stir bar during the laser irradiation with a stirring speed of  $3.0 \times 10^2$  rpm measured by a hand tachometer (HT-4200; Ono Sokki). Absorption spectroscopy was carried out 30 s after the laser irradiation experiment to avoid the interference by bubbles formed in solution with a JASCO V-750iRM or V-750ST spectrophotometer. We placed slits (height 1 mm, width 9 mm) both the reference and sample optical paths of the spectrophotometer to observe only the central part of the cuvette filled with 1 cm<sup>3</sup> solution. Molar absorption coefficient of  $\text{Eu}^{2+}$  in water was determined in degassed aqueous  $\text{EuCl}_2$  solution, which was prepared by dissolving  $\text{EuCl}_2$  in degassed water in a vacuum line.

The time evolution of the transmittance was measured by using a diode laser (635 nm) and a calibrated Si pin-photodiode. A pinhole (600  $\mu\text{m}$  in diameter) was placed in both the front and back of the cuvette. The output signal from a Si pin-photo diode was collected by using a data logger (Graphtec, GL820). To avoid any disturbance caused by bubbles, the transmittance measurements of the solution (3  $\text{cm}^3$ ) were carried out 30 s after the stirring was stopped. For the preparation of specimens for emission spectroscopy, the solution was centrifuged repeatedly (1.00 $\times 10^4$  rpm, 10 min). After removing the water, the residuals were sonicated in distilled water followed by centrifugation. This procedure was repeated three times. The precipitates were then separated from water by centrifugation followed by drying in a vacuum. The corrected emission spectrum of the precipitates excited at 290 nm was measured by a Hitachi F-7000 spectrofluorometer.

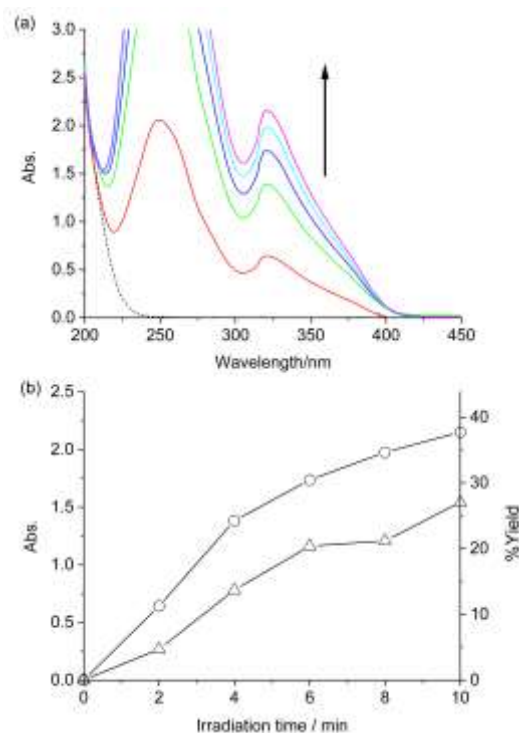
### 3. Results

#### 3.1. *Reduction of europium ions by femtosecond laser pulses*

Figure 2a shows the absorption spectral changes of  $\text{EuCl}_3$  aqueous solution upon laser irradiation. Before laser irradiation, the trailing edge of the charge-transfer (CT) band ( $\text{Eu}^{3+}$  and water) peaking in the VUV region was observed [26]. Two peaks centered at 248 and 320 nm appeared after the laser irradiation. These characteristic peaks were assigned to be the transition of  $4f^7 \rightarrow 4f^6 5d^1$  of  $\text{Eu}^{2+}$  [27]. The time evolution of the absorbance of  $\text{Eu}^{2+}$  at 320 nm is shown in Fig. 2b. It is noted that the absorbance was not changed on the time scale of absorption spectrum measurements (3 min). The production of  $\text{Eu}^{2+}$  seems to be linearly proportional to the laser irradiation time up to 4 min and then saturated by both the 200 and 400 mW laser pulses. The linear increase of  $\text{Eu}^{2+}$  is understood that the production of reductant, i.e., hydrated electrons is linearly

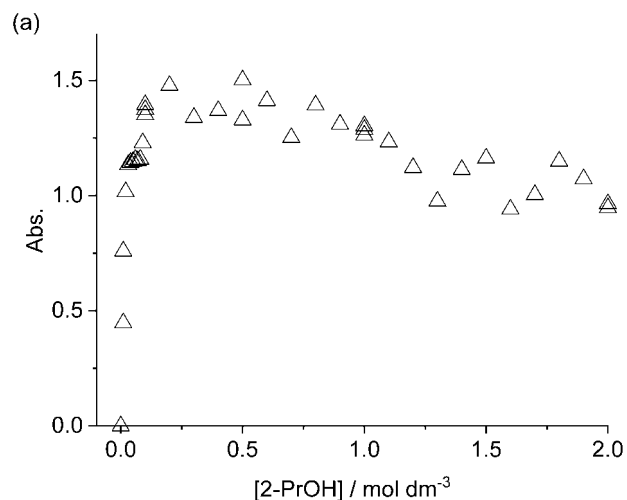
dependent of the laser irradiation time since the amount of water, solvent, is sufficient. However, equilibrium between  $\text{Eu}^{3+}$  and  $\text{Eu}^{2+}$  causes the saturation of  $\text{Eu}^{2+}$  production because the reaction volume is small ( $1 \text{ cm}^3$ ). In order to estimate the reduction yield, we determined the molar absorption coefficient of  $\text{EuCl}_2$  in water. To investigate the molar absorption coefficient of  $\text{Eu}^{2+}$  in water, the absorption spectrum of the  $\text{EuCl}_2$  in degassed methanol was measured successively after the measurement of that in degassed water. The amount of  $\text{EuCl}_2$  and the volume of solution are same between the two runs. We assume that the molar absorption coefficient of  $\text{EuCl}_2$  in methanol is the same as the reported molar absorption coefficient of  $\text{EuBr}_2$  in methanol ( $556 \text{ dm}^3 \text{ mol}^{-1} \text{ cm}^{-1}$  at 330 nm) [28]. The evaluated molar absorption coefficient of  $\text{EuCl}_2$  in degassed water ( $5.7 \times 10^2 \text{ dm}^3 \text{ mol}^{-1} \text{ cm}^{-1}$  at 320 nm) was comparable to that measured for  $\text{EuCl}_2$  in acidic water ( $5.0 \times 10^2 \text{ dm}^3 \text{ mol}^{-1} \text{ cm}^{-1}$  at 320 nm,  $\text{pH} = 1$ ) [29]. For the 10-min laser irradiation with maximum laser power (400 mW) used in this study, the conversion yields of  $\text{Eu}^{2+}$  was calculated to be 38% as shown in Fig. 2b.





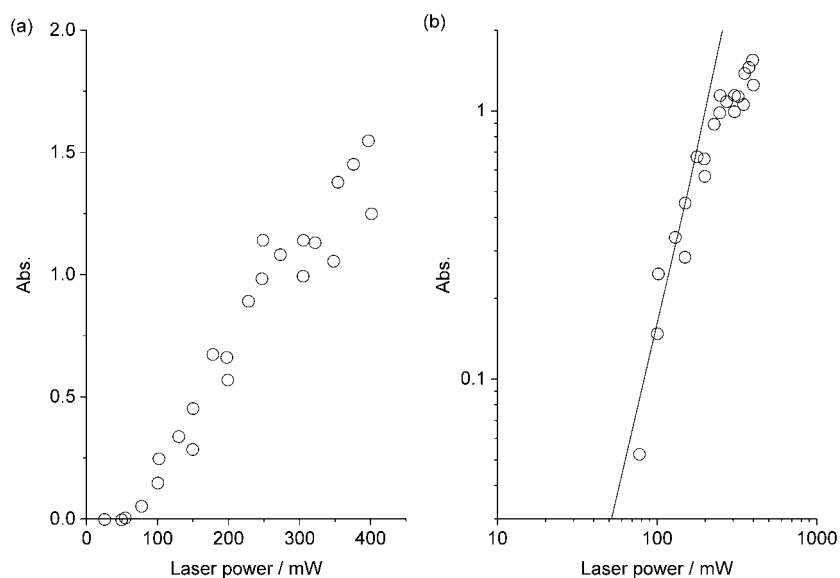
**Fig. 2.** (a) Absorption spectra of  $\text{EuCl}_3$  (10 mM, 1 cm<sup>3</sup>) aqueous solution before (dotted line) and after (solid lines) the laser irradiation in the presence of 1.0 M 2-PrOH. The laser power was 400 mW. Laser irradiation times from top to bottom were 10, 8, 6, 4, and 2 min, respectively. (b) Time evolution of the absorbance of  $\text{Eu}^{2+}$  at 320 nm upon laser irradiation in the presence of 1.0 M 2-PrOH. The laser power was 200 (triangles) or 400 mW (circles).

Figure 3 shows the correlation between the absorbance of  $\text{Eu}^{2+}$  and the initial concentration of 2-PrOH under the fixed laser irradiation condition (400 mW, 4 min). In order to compare the production yields, the data obtained for the 4-min laser irradiation were used to avoid the saturation effect observed in Fig. 2b. The reduction of  $\text{Eu}^{3+}$  did not occur in the absence of 2-PrOH. The production of  $\text{Eu}^{2+}$  steeply increased as the concentration of 2-PrOH increased. The absorbance became maximal at around 0.2 M of 2-PrOH, and then slightly decreased as the initial concentration of 2-PrOH increased.



**Fig. 3.** The correlation between the absorbance of  $\text{Eu}^{2+}$  (320 nm) after the exposure of  $\text{EuCl}_3$  aqueous solution (10 mM, 1  $\text{cm}^3$ ) to laser pulses for 4 min and the initial concentration of 2-PrOH. The laser power was 400 mW. Batch-type experiments were performed.

We then examined the effect of laser power on the yields of the production of  $\text{Eu}^{2+}$  in the presence of 0.2 M 2-PrOH (Fig. 4a). There was a threshold of  $\text{Eu}^{2+}$  formation, and then the yield of  $\text{Eu}^{2+}$  was steeply increased and saturated as the laser power increased. As seen in the log-log form of Fig. 4a, the production of  $\text{Eu}^{2+}$  was considered to be proportional to the cubic of the laser power (Fig. 4b). For the determination of the effect of laser power on the production rate of  $\text{Eu}^{2+}$ ,  $\text{EuCl}_3$  aqueous solutions (3  $\text{cm}^3$ ) were used to avoid the saturation effect as observed in Fig. 2b. Figure 5a shows the least-squares fit of the time evolution of the absorbance of  $\text{Eu}^{2+}$  at various laser powers. There was a threshold of the production rate of  $\text{Eu}^{2+}$ , and the production rates were linearly proportional to the laser power (Fig. 5b).



**Fig. 4.** Laser-intensity dependencies presented in (a) linear-linear and (b) log-log scale for the absorbance of  $\text{Eu}^{2+}$  at 320 nm. An aqueous  $\text{EuCl}_3$  solution (10 mM, 1  $\text{cm}^3$ ) in the presence of 2-PrOH (0.2 M) was exposed to femtosecond laser pulses for 4 min. Batch-type experiments were performed. The line in (b) having slope 3.0 is shown to guide the eyes.

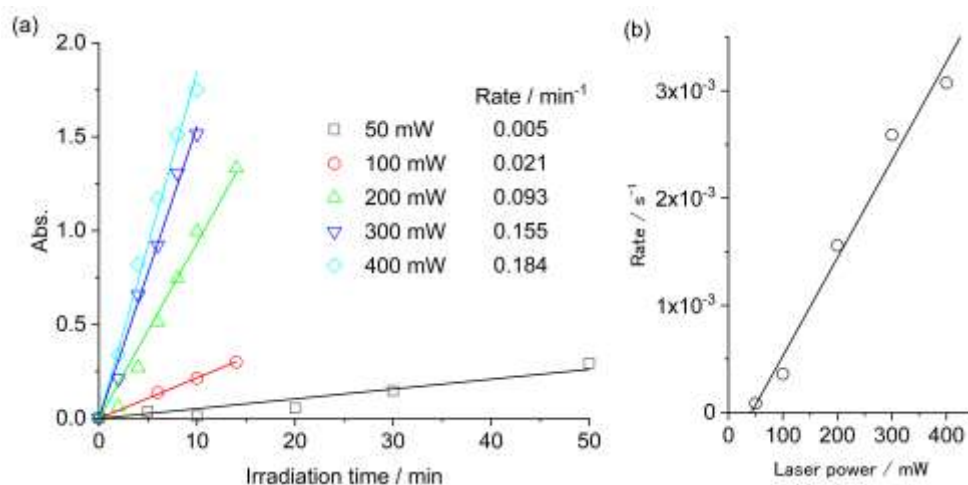


**Fig. 5.** (a) Time evolution of the absorbance of an aqueous  $\text{EuCl}_3$  (10 mM, 3  $\text{cm}^3$ ) solution at 320 nm upon laser irradiation in the presence of 2-PrOH (0.2 M). The straight lines are least-squares fits to obtain the rates of  $\text{Eu}^{2+}$  formation. (b) The rate of  $\text{Eu}^{2+}$  formation as a function of laser power. The line in (b) is shown to guide the eyes.

### ***3.2. Precipitation of europium ions in the presence of $SO_4^{2-}$***

Since divalent europium was sufficiently formed in the presence of 2-PrOH, we examined the precipitation of  $Eu^{2+}$  as sulfate. Figure 6a shows the appearance of the cuvette of  $EuCl_3$  aqueous solution in the presence of 2-PrOH (0.2 M) and  $(NH_4)_2SO_4$  (0.2 M). Before the laser irradiation, the peak of CT band between  $Eu^{3+}$  and  $SO_4^{2-}$  was clearly observed at 235 nm (Fig. 6b). Upon laser irradiation, violet-colored light emitted like a filament was clearly visible (Fig. 6a, 2 min). Such filaments result from the balance between self-focusing by a nonlinear refractive index of water and defocusing by plasma [30]. At the same time, a strong white-light emission was observed coaxially behind the filament. As the irradiation time increased, many bubbles illuminated by white light could be clearly observed (Fig. 6a, 4 min). In addition, the solution seemed to be white due to strong light scattering with 400 mW laser power irradiation. It can also be observed that the white-light spread at a high angle after the filament. At 6- and 8-min laser irradiation, the solution became homogeneous and the angle of the spread of white-light seemed to be larger under a high laser power condition. After the laser irradiation, the absorption spectrum showed the scattering component in the whole visible region due to the formation of precipitates (Fig. 6b). We thus collected the precipitates for the emission measurements. The peak wavelength of the emission of dried precipitates was 380 nm, which was within the range of the emission peak of the other divalent europium compounds ( $EuS$ , 350 nm [31];  $EuO$ , 357 nm [32];  $EuSe$ , 403 nm [33];  $EuCl_2$ , 404 nm [34]).

Figure 6b shows the absorption spectral changes during the laser irradiation with the power of 200 mW. After 4 min laser irradiation, the characteristic absorption of  $Eu^{2+}$  was observed, while the scattering component was negligible. Based on the

absorbance, the production of  $\text{Eu}^{2+}$  was not significantly affected by the presence of sulfate ions. As clearly shown in Fig. 6c, we cannot identify the presence of  $\text{EuSO}_4$  by absorption spectroscopy because the absorption spectrum taken after 4-min laser irradiation in the presence of sulfate ions (green) was identical to that reconstructed with those of  $\text{Eu}^{3+}$  taken before laser irradiation (red) and of  $\text{Eu}^{2+}$  aqueous solution without sulfate ions (blue, Fig. 2a). We concluded that the reduction of  $\text{Eu}^{3+}$  definitely occurred, but the concentration of  $\text{Eu}^{2+}$  was not sufficient to form precipitates. However, it is emphasized that the characteristic absorption and/or extinction spectrum was observed after 6-min laser irradiation. The peak of  $\text{Eu}^{2+}$  was slightly increased, while a very broad peak centered at around 450 nm clearly appeared. The appearance of a characteristic broad peak in visible region and its red-shift in the extinction spectrum were reported for submicrometer spheres of  $\text{TiO}_2$  [35]. If we refer to the linear relationship that the peak wavelength was 1.5 times larger than the size of the sphere, the size of spheres appeared after 6-min laser irradiation is estimated to be 300 nm. Additional 2-min laser irradiation resulted in the appearance of baseline components attributed to light scattering in the whole visible region. However, we could still recognize a hump centered at around 650 nm, which corresponds to the sphere size of 430 nm. It is mentioned that the contribution of  $\text{Eu}^{2+}$  at 8-min laser irradiation became smaller than those observed after 6-min laser irradiation. Therefore, the decrease in the  $\text{Eu}^{2+}$  peak is attributed to the formation of precipitates. Unfortunately, we could not determine the actual concentrations of  $\text{Eu}^{2+}$  and  $\text{Eu}^{3+}$  by absorption spectroscopy when precipitation starts, because complicated peak analyses including scattering components are required for this determination. Further laser irradiation did not increase the absorption

(extinction) of the solution, indicating that the reaction reached equilibrium or became inefficient due to light scattering.

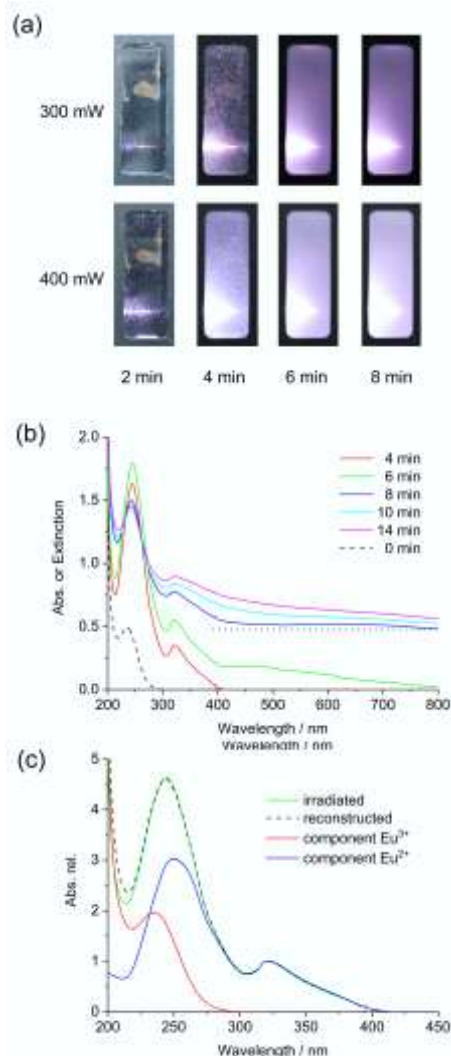


**Fig. 6.** (a) The appearance of the cuvette after the 2, 4, 6, and 8-min laser irradiation to  $\text{EuCl}_3$  aqueous solution (10 mM, 3  $\text{cm}^3$ ) in the presence of 2-PrOH (0.2 M) and  $(\text{NH}_4)_2\text{SO}_4$  (0.2 M). The laser power was 300 (upper panels) or 400 mW (lower panels). The solution was stirred during the laser irradiation. The brightness of the pictures taken after the 2-min laser irradiation was increased for better visibility. (b) Absorption spectra before (dashed line) and after the 4, 6, 8, 10, and 14-min laser irradiation (solid lines). The laser power was 200 mW. The dotted horizontal line is shown to indicate a baseline for the spectrum taken after 8-min laser irradiation. (c) Absorption spectra of  $\text{EuCl}_3$  aqueous solution in the presence of 2-PrOH (0.2 M) and  $(\text{NH}_4)_2\text{SO}_4$  (0.2 M). The absorption spectrum of  $\text{EuCl}_3$  aqueous solution after 4-min laser irradiation (200 mW,

green) reproduced by that of  $\text{Eu}^{3+}$  taken before laser irradiation (red) and that of  $\text{Eu}^{2+}$  taken in the absence of  $(\text{NH}_4)_2\text{SO}_4$  (blue). The reconstructed spectrum is shown as a dashed line.

Since the time to formation of white precipitates was dependent on the laser power, as observed in Fig. 6a, the time evolutions of the transmittance of the solution irradiated at various laser powers were measured. Figure 7 clearly shows that the transmittance was suddenly dropped after a certain induction time. Moreover, the induction time was shortened by increasing the laser power. After the sudden drop, the transmittance appeared to remain constant at 50 mW laser power, whereas the transmittance gradually decreased with a long decay rate under a high laser power condition ( $>100$  mW). The gradually decreased component of transmittance might have been mainly related to the decrease of the reduction efficiency due to the light-scattering. Herein, we compared the laser power and induction time. The induction time is defined as the time during which no reaction occur and the transmittance is kept to 100% in this experiment. In addition, residual transmittance, which is defined as the transmittance at twice the induction time, was also compared. Induction times and residual transmittances are listed in Table 1. In order to investigate the correlation between the induction time and the laser power, we used the reciprocal of induction time as a pseudo-rate. The reciprocal of induction time was linearly proportional to laser power as shown in Fig. 7b. As for the residual transmittance, interpretation was difficult because the transmittance is determined by various factors such as the size of precipitate. Nonetheless, the residual transmittance was decreased as the laser power increased.

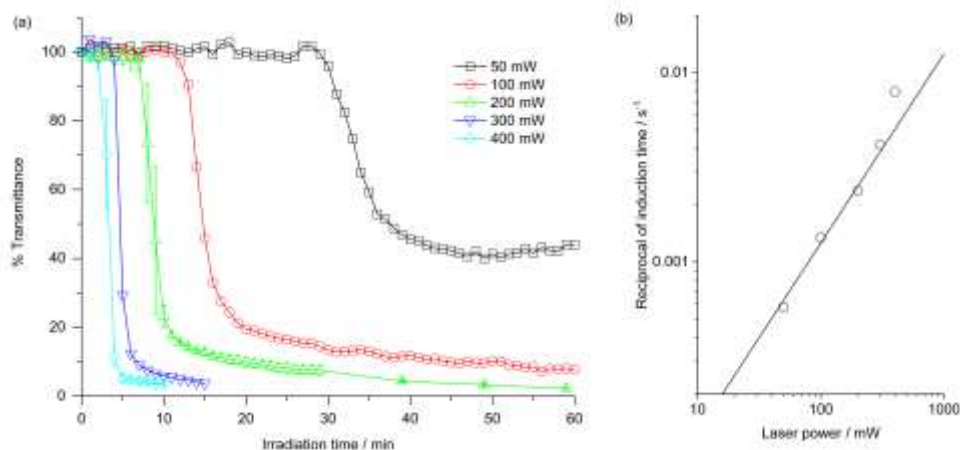


**Fig. 7.** (a) Time evolution of the transmittance of aqueous  $\text{EuCl}_3$  ( $10 \text{ mM}$ ,  $3 \text{ cm}^3$ ) solution at  $635 \text{ nm}$  upon laser irradiation in the presence of  $2\text{-PrOH}$  ( $0.20 \text{ M}$ ) and  $(\text{NH}_4)_2\text{SO}_4$  ( $0.20 \text{ M}$ ). The laser power was  $50$  (squares),  $100$  (circles),  $200$  (triangles),  $300$  (inverted triangles), and  $400 \text{ mW}$  (diamonds), respectively. The vertical bars give the standard deviation obtained for three different samples. (b) The correlation between the reciprocal of induction time and laser power. The line in (b) having slope  $1.0$  is shown to guide the eyes.

**Table 1** Induction time and residual transmittance

Laser power / $\text{mW}^a$	Induction time / min	%Residual transmittance
50	28.9	42.2
100	12.4	16.6
200	7.0	13.6
300	4.0	8.3
400	2.1	8.4

<sup>a</sup> Standard deviation of the laser power was about  $\pm 1.5\%$ .

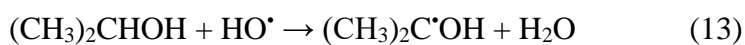
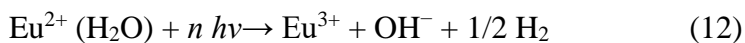
#### 4. Discussion

We have achieved near-infrared femtosecond laser-induced reduction of lanthanoid ions ( $\text{Eu}^{3+}$ ,  $\text{Sm}^{3+}$ ,  $\text{Yb}^{3+}$ ) in degassed alcohol [21-23]. In degassed alcohol, solvated electrons



would be a dominant reductant formed by nonresonant multiphoton ionization using femtosecond laser pulses. In contrast to the experiments in alcohol, many active species are formed in water. The primary reactions (1) to (5) in water are expected to be similar regardless of the excitation/ionization methods, which include radiolysis, discharges, or photolysis [36]. The reactive intermediates formed in the primary reactions are hydrated electron ( $e^-_{aq}$ ), hydrogen radical ( $H^\cdot$ ), and hydroxyl radical ( $HO^\cdot$ ). The former two would act as reductants and  $HO^\cdot$  should be an oxidant. Therefore, the competition between reduction and oxidation determines the total reaction efficiency. For example, carbon nanoparticles are formed by the oxidation of benzene with hydroxyl radicals [37, 38], whereas reduction by solvated electrons is a dominant primary reaction to form carbon nanoparticles in the case of halogenated molecules [39, 40]. For the reduction of  $Eu^{3+}$ , hydrated electrons rather than hydrogen radicals play a dominant role, since the excitation (2) that is the origin of hydrogen radical (5) is dominated by the ionization (1). In contrast to the case of degassed alcohol, in which recombination would be a major deactivation path of solvated electron, hydrated electrons are dominantly quenched by oxygen in aerated water (6). However, the lifetime of hydrated electrons was reported to be 0.3  $\mu s$  under an aerated condition [36]. The reduction of  $Eu^{3+}$  by a hydrated electron is an exergonic reaction (7) based on the reduction potentials of  $Eu^{3+}$  ( $-0.35$  V vs. SHE) [41] and hydrated electron ( $-2.87$  V vs. SHE) [42]. We can expect that the reduction of  $Eu^{3+}$  (10 mM) by a hydrated electron (7) rather than by hydrogen radicals (8) occurs at a diffusion-controlled rate ( $6.1 \times 10^{10} \text{ mol}^{-1} \text{ dm}^3 \text{ s}^{-1}$ ) [43, 44]. However, the re-oxidation of  $Eu^{2+}$  by oxygen (10) occurs, since the reduction potential of oxygen is  $-0.18$  V vs. SHE (in water) [45]. This re-oxidation might be a serious issue, because the solution is saturated by oxygen evolved in water exposed to femtosecond laser pulses [46]. A more

serious problem is the generation of hydroxyl radical, which is a strong oxidant formed in water and which reacts with  $\text{Eu}^{2+}$  (11). In addition, the multiphoton excitation of  $\text{Eu}^{2+}$  will reproduce  $\text{Eu}^{3+}$  (12), as observed in alcohol [21]. The re-oxidation processes (10) and (12) cannot be avoided. In contrast, the addition of a hydroxyl radical scavenger (13), 2-PrOH, was very effective to produce  $\text{Eu}^{2+}$ , as clearly shown in Fig. 3. The production of  $\text{Eu}^{2+}$  was maximized when the concentration of 2-PrOH was about 20 times larger than that of  $\text{EuCl}_3$ , but the efficiency was gradually decreased as the concentration of 2-PrOH was increased. Therefore, it was suggested that 2-PrOH radical might not act as an important reductant of  $\text{Eu}^{3+}$  (9) under our experimental condition.





The presence of induction time before precipitation starts was reported in the cases of UV lamp excitation experiments; however, the information about the valence of Eu during induction time was not obtained [8]. In this study, we showed that  $\text{Eu}^{2+}$  was clearly observed during the induction time even in the presence of sulfate ions (Fig. 6b). Moreover, the absorption spectrum of  $\text{Eu}^{2+}$  in the presence of sulfate ions was identical to that without sulfate ions (Fig. 6c). Since the concentrations of  $\text{Eu}^{2+}$  and  $\text{SO}_4^{2-}$  are sufficient to form  $\text{EuSO}_4$ , we expect that reaction (14) occurs at the beginning of the laser irradiation and speculate that the absorption spectrum of  $\text{Eu}^{2+}$  coordinated by sulfate ions is not strongly affected by the coordination of sulfate ions or identical to that of  $[\text{Eu}(\text{H}_2\text{O})_7]^{2+}$  [47]. Consequently, the linear relationship between the reciprocal of induction time and laser power suggests that agglomeration process (15) is rate-determining step of precipitation. Agglomerates of several hundreds of nanometers were identified by their resonant scattering wavelength just before the precipitation starts (at 6 min in Fig. 6b). Thus,  $\text{Eu}^{2+}$  would coexist as an ion and as agglomerated  $\text{EuSO}_4$  of few to tens of nanometers in size at the early stage of induction time. The former is detected by its characteristic absorption peak at 320 nm, but the latter is invisible in the ultraviolet and visible wavelength region. In order to investigate what actually occurs during the induction time, in situ dynamic light scattering and X-ray absorption near edge structure measurements would be helpful [48].

## 5. Conclusion

This work reveals that the reactive species generated in water by femtosecond laser pulses can reduce europium ions even under an aerated condition. The absence of oxygen is not the critical factor, but hydroxyl radical scavengers are indispensable to achieve the reduction of europium ions. We performed the precipitation of europium sulfate in this study, but some lingering issues will need to be resolved to achieve the collection of lanthanoid ions from water. First, in our experiments the efficiency of reduction was saturated, probably due to the back reaction induced by multiphoton excitation of  $\text{Eu}^{2+}$ . A possible solution to this problem would be to use the laser pulse of the wavelength longer than  $0.8 \mu\text{m}$ . Second, the efficiency of precipitation was decreased as observed by the transmittance measurements. This is a fundamental problem of batch-type experiments, and thus a flow-system or removal of precipitates by filtering and/or centrifugation is required to improve the precipitation procedure. Third, the induction time of the precipitation was shortened by femtosecond laser pulses, but is still a few minutes. We revealed that the reciprocal of the induction time is linearly proportional to the laser power. Therefore, one way to shorten the induction time would be to increase the laser power, but a more effective approach would be to use high-repetition laser pulses. We could use a high-repetition ( $>1 \text{ MHz}$ ) picosecond laser, which is a compact, reasonable, and industrially robust device. The use of such a laser would diminish the induction time of precipitation. The combination of a high-repetition laser and a flow system would be a key approach for the recycling metal ions.

## **Acknowledgments**

The present research was supported by Takahashi Industrial and Economic Research Foundation (11-003-142) and the Masuya Memorial Basic Research Foundation (202004).

## References

- [1] J.J.M. Nelson, E.J. Schelter, Sustainable Inorganic Chemistry: Metal Separations for Recycling, *Inorg. Chem.*, 58 (2019) 979-990.
- [2] A. Kumari, M.K. Jha, D.D. Pathak, S. Chakravarty, J.C. Lee, Processes developed for the separation of europium (Eu) from various resources, *Sep. Purif. Rev.*, 48 (2019) 91-121.
- [3] F. Xie, T.A. Zhang, D. Dreisinger, F. Doyle, A critical review on solvent extraction of rare earths from aqueous solutions, *Miner. Eng.*, 56 (2014) 10-28.
- [4] T. Donohue, Laser Purification of the Rare-Earths, *Opt. Eng.*, 18 (1979) 181-186.
- [5] B.B. Mishra, N. Devi, K. Sarangi, Yttrium and europium recycling from phosphor powder of waste tube light by combined route of hydrometallurgy and chemical reduction, *Miner. Eng.*, 136 (2019) 43-49.
- [6] B. Van den Bogaert, L. Gheeraert, M.E. Leblebici, K. Binnemans, T. Van Gerven, Photochemical recovery of europium from non-aqueous solutions, *Phys. Chem. Chem. Phys.*, 18 (2016) 29961-29968.
- [7] T. Donohue, Photochemical separation of europium from lanthanide mixtures in aqueous solution, *J. Chem. Phys.*, 67 (1977) 5402-5404.
- [8] B. Van den Bogaert, L. Van Meerbeeck, K. Binnemans, T. Van Gerven, Influence of irradiance on the photochemical reduction of europium(III), *Green Chem.*, 18 (2016) 4198-4204.
- [9] B. Van den Bogaert, D. Havaux, K. Binnemans, T. Van Gerven, Photochemical recycling of europium from Eu/Y mixtures in red lamp phosphor waste streams, *Green Chem.*, 17 (2015) 2180-2187.
- [10] Y.F. Wu, Q.J. Zhang, T.Y. Zuo, Selective recovery of Y and Eu from rare-earth tricolored phosphorescent powders waste via a combined acid-leaching and photo-reduction process, *J. Clean Prod.*, 226 (2019) 858-865.
- [11] S.C. Li, S.C. Kim, C.S. Kang, C.J. Kim, C.J. Kang, Separation of samarium, europium and gadolinium in high purity using photochemical reduction-extraction chromatography, *Hydrometallurgy*, 178 (2018) 181-187.

- [12] T. Hirai, N. Onoe, I. Komasa, Separation of Europium from Samarium and Gadolinium by Combination of Photochemical Reduction and Solvent Extraction, *J. Chem. Eng. Jpn.*, 26 (1993) 64-67.
- [13] M. Kusaba, N. Nakashima, W. Kawamura, Y. Izawa, C. Yamanaka, Higher Yield of Photoreduction from  $\text{Eu}^{3+}$  to  $\text{Eu}^{2+}$  with Shorter Wavelength Irradiation, *Chem. Phys. Lett.*, 197 (1992) 136-140.
- [14] M. Kusaba, N. Nakashima, W. Kawamura, Y. Izawa, C. Yamanaka, High Photoreduction Yield of  $\text{Eu}^{3+}$  to  $\text{Eu}^{2+}$  in Alcoholic Solutions and Its Wavelength Dependence, *J. Alloys Compd.*, 192 (1993) 284-286.
- [15] M. Saeki, T. Taguchi, N. Nakashima, H. Ohba, Wet separation between palladium(II) and molybdenum(IV) ions by using laser-induced particle formation: Enhancement of recovery efficiency of palladium by laser condition, *J. Photochem. Photobiol. A*, 299 (2015) 189-193.
- [16] S. Asai, T. Yomogida, M. Saeki, H. Ohba, Y. Hanzawa, T. Horita, Y. Kitatsuji, Determination of  $^{107}\text{Pd}$  in Pd Recovered by Laser-Induced Photoreduction with Inductively Coupled Plasma Mass Spectrometry, *Anal. Chem.*, 88 (2016) 12227-12233.
- [17] S. Asai, M. Ohata, T. Yomogida, M. Saeki, H. Ohba, Y. Hanzawa, T. Horita, Y. Kitatsuji, Determination of  $^{107}\text{Pd}$  in Pd purified by selective precipitation from spent nuclear fuel by laser ablation ICP-MS, *Anal. Bioanal. Chem.*, 411 (2019) 973-983.
- [18] M. Saeki, D. Matsumura, T. Yomogida, T. Taguchi, T. Tsuji, H. Saitoh, H. Ohba, In Situ Time-Resolved XAFS Studies on Laser-Induced Particle Formation of Palladium Metal in an Aqueous/EtOH Solution, *J. Phys. Chem. C*, 123 (2019) 817-824.
- [19] M. Kusaba, N. Nakashima, Y. Izawa, C. Yamanaka, W. Kawamura, Two-photon reduction of  $\text{Eu}^{3+}$  to  $\text{Eu}^{2+}$  via the  $f \leftarrow f$  transitions in methanol, *Chem. Phys. Lett.*, 221 (1994) 407-411.
- [20] N. Nakashima, S. Nakamura, S. Sakabe, H. Schillinger, Y. Hamanaka, C. Yamanaka, M. Kusaba, N. Ishihara, Y. Izawa, Multiphoton Reduction of  $\text{Eu}^{3+}$  to  $\text{Eu}^{2+}$  in Methanol Using Intense, Short Pulses from a Ti:Sapphire Laser, *J. Phys. Chem. A*, 103 (1999) 3910-3916.
- [21] D. Nishida, M. Kusaba, T. Yatsushashi, N. Nakashima, Reduction of  $\text{Eu}^{3+}$  to  $\text{Eu}^{2+}$  by an intense femtosecond laser pulse in solution, *Chem. Phys. Lett.*, 465 (2008) 238-240.
- [22] D. Nishida, E. Yamade, M. Kusaba, T. Yatsushashi, N. Nakashima, Reduction of  $\text{Sm}^{3+}$  to  $\text{Sm}^{2+}$  by an Intense Femtosecond Laser Pulse in Solution, *J. Phys. Chem. A*, 114 (2010) 5648-5654.
- [23] N. Nakashima, K. Yamanaka, A. Itoh, T. Yatsushashi, Ionic Valence Change of Metal Ions in Solution by Femtosecond Laser Excitation Accompanied by White-Light Laser,

Chin. J. Phys., 52 (2014) 504-518.

[24] N. Nakashima, K. Yamanaka, M. Saeki, H. Ohba, S. Taniguchi, T. Yatsunami, Metal ion reductions by femtosecond laser pulses with micro-Joule energy and their efficiencies, *J. Photochem. Photobiol. A*, 319 (2016) 70-77.

[25] T. Okamoto, T. Nakamura, K. Sakota, T. Yatsunami, Synthesis of Single-Nanometer-Sized Gold Nanoparticles in Liquid-Liquid Dispersion System by Femtosecond Laser Irradiation, *Langmuir*, 35 (2019) 12123-12129.

[26] Y. Haas, G. Stein, M. Tomkiewi, Fluorescence and Photochemistry of Charge-Transfer Band in Aqueous Europium(III) Solutions, *J. Phys. Chem.*, 74 (1970) 2558-2562.

[27] J. Jiang, N. Higashiyama, K. Machida, G. Adachi, The luminescent properties of divalent europium complexes of crown ethers and cryptands, *Coord. Chem. Rev.*, 170 (1998) 1-29.

[28] G. Adachi, N. Higashiyama, Luminescence of Europium(II) Complexes with Crown Compounds, *Nippon Kagaku Kaishi*, (1993) 418-432.

[29] M. Brandys, G. Stein, Photochemical Evolution of Hydrogen from Aqueous Solutions of Europium Ions at  $\lambda > 310$  nm. The Role of Europium(II), *J. Phys. Chem.*, 82 (1978) 852-854.

[30] S.L. Chin, S.A. Hosseini, W. Liu, Q. Luo, F. Theberge, N. Akozbek, A. Becker, V.P. Kandidov, O.G. Kosareva, H. Schroeder, The propagation of powerful femtosecond laser pulses in optical media: physics, applications, and new challenges, *Can. J. Phys.*, 83 (2005) 863-905.

[31] Y. Hasegawa, Y. Okada, T. Kataoka, T. Sakata, H. Mori, Y. Wada, Synthesis and photophysical properties of EuS nanoparticles from the thermal reduction of novel Eu(III) complex, *J. Phys. Chem. B*, 110 (2006) 9008-9011.

[32] Y. Hasegawa, S. Thongchant, Y. Wada, H. Tanaka, T. Kawai, T. Sakata, H. Mori, S. Yanagida, Enhanced luminescence and photomagnetic properties of surface-modified EuO nanocrystals, *Angew. Chem. Int. Ed.*, 41 (2002) 2073-2075.

[33] C.X. Wang, D. Zhang, L. Xu, Y.G. Jiang, F.X. Dong, B. Yang, K. Yu, Q. Lin, A Simple Reducing Approach Using Amine To Give Dual Functional EuSe Nanocrystals and Morphological Tuning, *Angew. Chem. Int. Ed.*, 50 (2011) 7587-7591.

[34] W.L. Jiang, Z.Q. Bian, C.M. Hong, C.H. Huang, A Mild Liquid Reduction Route toward Uniform Blue-Emitting EuCl<sub>2</sub> Nanoprisms and Nanorods, *Inorg. Chem.*, 50 (2011) 6862-6864.

[35] H.Q. Wang, M. Miyauchi, Y. Ishikawa, A. Pyatenko, N. Koshizaki, Y. Li, L. Li, X.Y. Li, Y. Bando, D. Golberg, Single-Crystalline Rutile TiO<sub>2</sub> Hollow Spheres: Room-Temperature Synthesis, Tailored Visible-Light-Extinction, and Effective Scattering Layer

- for Quantum Dot-Sensitized Solar Cells, *J. Am. Chem. Soc.*, 133 (2011) 19102-19109.
- [36] C.L. Thomsen, D. Madsen, S.R. Keiding, J. Thogersen, O. Christiansen, Two-photon dissociation and ionization of liquid water studied by femtosecond transient absorption spectroscopy, *J. Chem. Phys.*, 110 (1999) 3453-3462.
- [37] T. Yatsunami, N. Uchida, K. Nishikawa, Novel Method of Producing Carbon Nanoparticles on Benzene/Water Interface with Femtosecond Laser Plasma Filament, *Chem. Lett.*, 41 (2012) 722-724.
- [38] T. Hamaguchi, T. Okamoto, K. Mitamura, K. Matsukawa, T. Yatsunami, Synthesis of Hydrophilic and Hydrophobic Carbon Nanoparticles from Benzene/Water Bilayer Solution with Femtosecond Laser Generated Plasma Filaments in Water, *Bull. Chem. Soc. Jpn.*, 88 (2015) 251-261.
- [39] T. Okamoto, K. Mitamura, T. Hamaguchi, K. Matsukawa, T. Yatsunami, Synthesis of Fluorine-Doped Hydrophilic Carbon Nanoparticles from Hexafluorobenzene by Femtosecond Laser Pulses, *ChemPhysChem*, 18 (2017) 1007-1011.
- [40] T. Okamoto, E. Miyasaka, K. Mitamura, K. Matsukawa, T. Yatsunami, Precipitation of dichloromethane as low-chlorine carbon nanoparticles from water by femtosecond laser pulses, *J. Photochem. Photobiol. A*, 344 (2017) 178-183.
- [41] L.B. Anderson, D.J. Macero, The Formal Reduction Potential of Europium(III)-Europium(II) System, *J. Phys. Chem.*, 67 (1963) 1942-1942.
- [42] A. Kumar, A. Adhikary, L. Shamoun, M.D. Sevilla, Do Solvated Electrons ( $e_{aq}^-$ ) Reduce DNA Bases? A Gaussian 4 and Density Functional Theory- Molecular Dynamics Study, *J. Phys. Chem. B*, 120 (2016) 2115-2123.
- [43] J.K. Thomas, S. Gordon, E.J. Hart, Rates of Reaction of Hydrated Electron in Aqueous Inorganic Solutions, *J. Phys. Chem.*, 68 (1964) 1524-1527.
- [44] M. Faraggi, Y. Tendler, Pulse Radiolysis in Lanthanide Aqueous-Solutions .1. Formation Spectrum and Chemical Properties of Divalent Europium, Ytterbium, and Samarium Ions, *J. Chem. Phys.*, 56 (1972) 3287-3293.
- [45] W.H. Koppenol, D.M. Stanbury, P.L. Bounds, Electrode potentials of partially reduced oxygen species, from dioxygen to water, *Free Radic. Biol. Med.*, 49 (2010) 317-322.
- [46] S.L. Chin, S. Lagace, Generation of H<sub>2</sub>, O<sub>2</sub>, and H<sub>2</sub>O<sub>2</sub> from water by the use of intense femtosecond laser pulses and the possibility of laser sterilization, *Appl. Opt.*, 35 (1996) 907-911.
- [47] G. Moreau, L. Helm, J. Purans, A.E. Merbach, Structural investigation of the aqueous Eu<sup>2+</sup> ion: Comparison with Sr<sup>2+</sup> using the XAFS technique, *J. Phys. Chem. A*, 106 (2002) 3034-3043.



[48] M. Van de Voorde, B. Geboes, T. Vander Hoogerstraete, K. Van Hecke, T. Cardinaels, K. Binnemans, Stability of europium(ii) in aqueous nitrate solutions, Dalton Trans., 48 (2019) 14758-14768.